

# Floquet Amorphous Topological Orders in a Rydberg Glass

Peng He,<sup>1,2,\*</sup> Jing-Xin Liu,<sup>3</sup> Hong Wu,<sup>4,†</sup> and Z. D. Wang<sup>1,2,‡</sup>

<sup>1</sup>*Guangdong-Hong Kong Joint Laboratory of Quantum Matter,  
Department of Physics, and HK Institute of Quantum Science & Technology,  
The University of Hong Kong, Pokfulam Road, Hong Kong, China*

<sup>2</sup>*Quantum Science Center of Guangdong-Hong Kong-Macau Great Bay Area, 3 Binlang Road, Shenzhen, China*

<sup>3</sup>*National Laboratory of Solid State Microstructures, School of Physics,  
and Collaborative Innovation Center of Advanced Microstructures, Nanjing University, Nanjing 210093, China*

<sup>4</sup>*School of Science, and Institute for Advanced Sciences,  
Chongqing University of Posts and Telecommunications, Chongqing 400065, China*

(Dated: April 30, 2024)

We study the Floquet amorphous topological orders in experimentally accessible one-dimensional array of randomly pointed Rydberg atoms with periodic driving. The filling factor in the chain is tunable by applying a microwave field. We give a complete characterization of the topological properties from both the single-particle and many-body aspect. The periodic driving results in richer topological phases. At the single-particle level, we calculate the real space winding numbers and polarization, confirming robust amorphous topological phases with 0-type and  $\pi$ -type edge modes. We show a structural disorder induced topological phase transition accompanied with localization transition in the nonequilibrium system. Furthermore, in the many-body case we find the existence of amorphous topological orders of the hardcore bosons half-filled the chain, in contrast described by the topological entanglement entropy and the string order. Possible detection methods are also addressed.

*Introduction.*—Symmetry-protected topological (SPT) orders have been widely explored in systems with underlying spatial order, such as topological insulators and superconductors [1–4], Dirac and Weyl semimetals [5, 6]. Nevertheless, it has been noted that the inclusion of the spatiotemporal engineering leads to richer topological phases. The SPT order can exist in systems without local crystalline symmetries, such as topological quasicrystals [7–10], amorphous solids and artificial materials with completely random sites [11–19]. Such topological glassy matter does not rely on the microscopic details of the spatial configuration, manifesting its robustness and facilitating the material fabrications. On another note, with an additional degree of freedom in the time domain, periodically driven nonequilibrium systems have extended the SPT phases to a new classification scheme, supporting anomalous bulk-boundary relations without equilibrium counterpart [20–25]. Aforementioned findings prompt a search for the new class of SPT phases with the synergy of Floquet topology and amorphous order. Meanwhile a feasible proposal on available quantum systems is in great need.

The studies of SPT orders usually focus on the fermionic systems. However, the SPT orders can naturally appear bosonic systems when strong interactions are considered and especially the hardcore condition is fulfilled [26–29]. The characterization and classification of the bosonic SPT phases are based on the ground state of the many-body systems. The concept of SPT orders has been extended to the nonequilibrium setup in terms of the Floquet quantum matter [30–36]. For the experimental aspect, the Rydberg atoms combined with Floquet engineering provide a versatile platform for the

quantum simulation of many-body physics and the topological theory, due to its high tunability [4, 37–42]. The Rydberg atoms are individually controlled by the optical tweezer [43–46], and the coupling is tunable via dipole-dipole and van der Waals interactions [47–49], which allows rather flexible and local design of the lattice configuration. Among various experimental progress [50–55], a bosonic SPT phase has been observed with a one-dimensional arrays of  $^{87}\text{Rb}$  atoms [50]. A later theoretical work has shown the existence of the bosonic SPT order in amorphous systems [56].

In this letter, we study the SPT phases in a one-dimensional (1D) Floquet amorphous bosonic Rydberg atomic array, based on a experimentally feasible setup. We show the existence of rich SPT phases in both the single-particle level and many-body level. In the single-particle level, we map out the phase diagram according to the real space winding number and the polarization. Topological 0 phase and  $\pi/T$  phase can exist in amorphous lattices with suitable design of the periodic drivings. Specifically, we further identify the structural disorder driven phase transitions in our model. We find clear numerical signatures of the Anderson localization in the topological regimes, implying a special gapless floquet phase. In the many-body level, we consider the hard core conditions at half-filling. We characterize the topology in terms of the topological entanglement entropy (TEE) and the string order, using exact diagonalization (ED) and density matrix renormalization group (DMRG). Furthermore, we provide methods to detect the SPT phases in the experiment, with either microwave spectroscopy or the edge fidelity, which extracts the nontrivial boundary physics related with the topology.

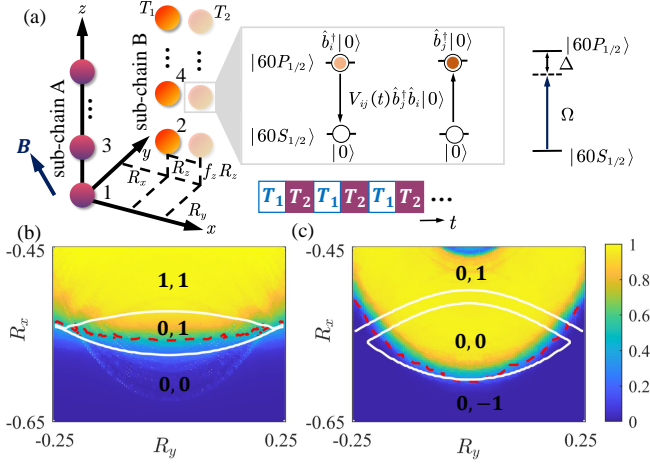


FIG. 1: (a) Schematics of the driving protocol on the array of Rydberg atoms with atoms at site  $2i-1$  and  $2i$  forming a unit cell. The two atoms in a unit cell are initially separated by a distance  $\mathbf{R} = (R_x, R_y, R_z)$ , and subject to a periodic modulation. The dipolar exchange interaction between two atoms provides hopping terms. The magnetic field  $\mathbf{B} = (-\sqrt{2}, 0, 1)B$  is applied in the  $x$ - $z$  plane with the polar angle  $\theta_m = \arccos(1/\sqrt{3})$  to cancel the hoppings within each subchain. The system is probed by a microwave field with the Rabi frequency  $\Omega$  and detuning  $\Delta$ . (b) Phase diagram characterized by  $N_0$ , with  $T_1 = T_2 = 0.4$ ,  $\mathbf{f} = (0.9, 1, 1)$ ,  $R_z = 0.72$ ,  $w = 0.8$ ,  $2L = 200$ . (c) Phase diagram characterized by  $N_\pi$ , with  $T_1 = T_2 = 0.4$ ,  $\mathbf{f} = (1, 1, 0.55)$ ,  $R_z = 0.8$ ,  $w = 0.8$ ,  $2L = 200$ . The numbers label the values of the winding numbers  $N_0$ ,  $N_\pi$  for a regular system. The red dashed lines show the phase boundaries determined by the polarization. The white solid lines show the phase boundaries of a regular system. All the quantities are averaged over 12 random configurations.

*Model Hamiltonian.*—We consider an array of  $2L$  individually trapped  $^{87}\text{Rb}$  atoms in a dimerized configuration, as shown in Fig. 1(a). For each atom, only two Rydberg states from the  $60S_{1/2}$  and the  $60P_{1/2}$  manifolds involve, which naturally serve as two distinct hard-core bosonic degrees of freedom. A s-level  $|60S_{1/2}, m_J = 1/2\rangle$  corresponds to the “vacuum” of the many-body system, and a p-level  $|60P_{1/2}, m_J = -1/2\rangle$  corresponds to one occupied boson. Because of the excitation transfer between two Rydberg atoms induced by the dipole-dipole interaction, the system is governed by the following Hamiltonian,

$$\hat{H}(t) = \sum_{i < j}^{2L} V_{ij}(t) (\hat{b}_i^\dagger \hat{b}_j + \hat{b}_j^\dagger \hat{b}_i), \quad (1)$$

where  $\hat{b}_i^\dagger$  ( $\hat{b}_i$ ) creates (annihilates) a hard-core boson at site  $i$ , and  $V_{ij} = \mathcal{d}_0^2(1 - 3\cos^2\theta_{ij})/R_{ij}^3$  is the dipolar coupling strength. Here  $\mathcal{d}_0$  is the dipole moment between the two sublevels,  $R_{ij}$  is the separation between the atoms at site  $i$  and site  $j$ , and its angle with respect to the magnetic field  $\mathbf{B}$  determines  $\theta_{ij}$ . Specifically, the two atoms in each unit cell are separated by

a vector  $\mathbf{R} = (R_x, R_y, R_z)a_0$ , and subject to an additional random displacement  $R_z^{2i-1} = (i-1 + \delta z_i)a_0$  and  $(R_z^{2i} = i-1 + R_z + \delta z_i)a_0$ , where  $\delta z_i$  is the structural disorder uniformly sampled in the range  $[-d/2, d/2]$ , amorously shaped the lattice geometry, and  $a_0$  is the lattice unit. When  $w = L$ , the system becomes completely random. Furthermore, the atoms in two subchains are aligned along the so-called “magic angle”  $\theta_{i+2} = \theta_m \equiv \arccos(1/\sqrt{3})$ , so that the coupling within each subchain is vanishing and the chiral (sublattice) symmetry is guaranteed. In following discussions, we set  $a_0 = 1$  and  $d^2/a_0^3$  as the units of length and energy, respectively, and set  $\hbar = 1$ .

To study the Floquet phases in this system, we consider the stroboscopic modulation of the atom displacement by periodically shift one of the subchain as,

$$\mathbf{R}(t) = \begin{cases} \mathbf{R}, & t \in [mT, mT + T_1) \\ \mathbf{f} \cdot \mathbf{R}, & t \in [mT + T_1, (m+1)T) \end{cases}, \quad m \in \mathbb{Z}, \quad (2)$$

where  $\mathbf{f} = (f_x, f_y, f_z)$  is a set of real coefficients. The dynamics is then described by the unitary evolution  $U_T = e^{-i\hat{H}_2 T_2} e^{-i\hat{H}_1 T_1}$ , where we denote the Hamiltonian the respective time duration  $T_1$  and  $T_2$  as  $\hat{H}_1$  and  $\hat{H}_2$  ( $T_2 \equiv T - T_1$ ). Then we have an effective Hamiltonian  $\hat{H}_F = \frac{i}{T} \ln U_T$ . The spectra  $\varepsilon_n$  of  $\hat{H}_F$  are known as quasienergies and we take  $\varepsilon_n \in [-\pi/T, \pi/T]$ .

We remark that the Hamiltonian  $\hat{H}(t)$  respects a dihedral  $\mathbb{Z}_2 \times \mathbb{Z}$  symmetry, represented by an anti-unitary operator  $\mathcal{S}_B = \prod_{i=1}^{2L} [b_i + b_i^\dagger]K$  and discrete translations in time ( $K$  denotes the complex conjugation). However,  $\hat{H}_F$  does not inherit the symmetry due to  $[\hat{H}_1, \hat{H}_2] \neq 0$ . After noting that  $U_T$  have a Floquet gauge degree of freedom, we can apply two similarity transformations  $\hat{G}_j = e^{i(-1)^j \hat{H}_j T_j/2}$ , converting  $U_T$  into  $\tilde{U}_{T,1} = e^{-i\hat{H}_1 T_1/2} e^{-i\hat{H}_2 T_2} e^{-i\hat{H}_1 T_1/2}$  and  $\tilde{U}_{T,2} = e^{-i\hat{H}_2 T_2/2} e^{-i\hat{H}_1 T_1} e^{-i\hat{H}_2 T_2/2}$  respectively, from which we define  $\tilde{H}_{F,i} = \frac{i}{T} \ln \tilde{U}_{T,i}$ .  $\tilde{H}_{F,i}$  share the same quasienergies as  $\hat{H}_T$ , but recover the symmetry of  $\hat{H}(t)$ .

Our model also preserves a  $U(1)$  symmetry  $[\hat{H}(t), \hat{N}] = 0$  with  $\hat{N} = \sum_i \hat{b}_i^\dagger \hat{b}_i$  being the total particle number operator thus  $\hat{N}$  is conserved. In the experiment, a weak global microwave field is applied to create a state with certain excitation numbers if the detuning matches the system energy [50]. Therefore, we can study this system at both single-particle level and many-body level.

*Single-particle case.*—We first study the topological properties of the single-excitation state manifold of the atom chain. We obtain a single-particle Hamiltonian  $\hat{H}_S(t)$  with  $[\hat{H}_S]_{ij} = V_{ij}(t)(1 - \delta_{ij})$  ( $1 \leq i, j \leq 2L$ ), under a basis  $\hat{b} \equiv \{\hat{b}_1^\dagger, \hat{b}_2^\dagger, \dots, \hat{b}_{2L}^\dagger\}$ .  $\hat{H}_S(t)$  is chiral symmetric  $S\hat{H}_S S^{-1} = -\hat{H}_S$  with  $S = \text{diag}\{(-1)^{j-1}\}_{j=1}^{2L}$ , thus is equivalent to a Floquet amorphous SSH model. The nontrivial Floquet topology manifests in the existence of zero-energy edge modes and  $\pi/T$ -energy edge modes, in

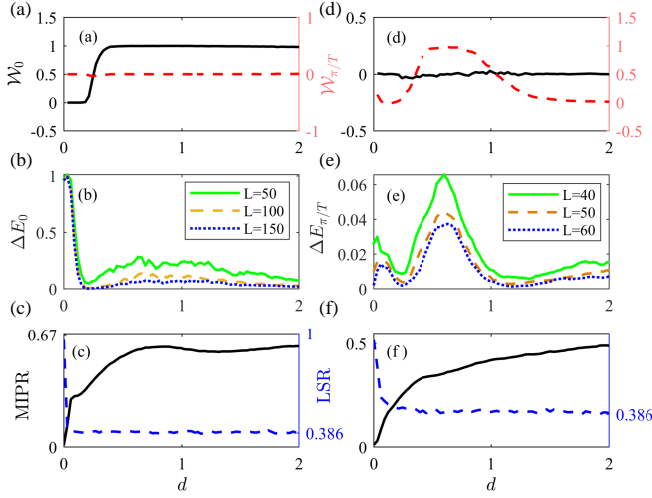


FIG. 2: The winding number (a), (d), quasienergy gap (b), (e), and MIPR and LSR (c), (f) versus structural disorder  $d$ . We use  $\mathbf{R} = (-0.5, 0, 0.8)$ ,  $\mathbf{f} = (0.9, 1, 1)$ ,  $T_1 = T_2 = 0.4$  for (a)-(c); and  $\mathbf{R} = (-0.5, 0, 0.8)$ ,  $\mathbf{f} = (1, 1, 0.55)$ ,  $T_1 = T_2 = 0.4$  for (d)-(f). All the quantities are averaged over 50 random configurations.

which the latter has no equilibrium counterpart.

In presence of the structural disorder, the quasimomentum is no longer a good quantum number. To characterize the topology of single particle bands, we calculate the real-space winding numbers [58–60],

$$\mathcal{W}'_j = \frac{1}{2L'} \text{Tr}'(SQ_j[Q_j, X]), \quad (3)$$

where  $X$  is the coordinate operator,  $Q_j = \sum_n (|n_j\rangle\langle n_j| - S|n_j\rangle\langle n_j|S^\dagger)$  with  $\hat{H}_{F,i}|n_j\rangle = \varepsilon_{j,n}|n_j\rangle$ , and  $\text{Tr}'$  denotes the trace over the bulk sites with length  $L' = L - 2\ell$ . The number of 0- and  $\pi/T$ -mode edge states relates to  $\mathcal{W}'_j$  as [61]

$$N_0 = (\mathcal{W}_1 + \mathcal{W}_2)/2, \quad N_{\pi/T} = (\mathcal{W}_1 - \mathcal{W}_2)/2. \quad (4)$$

The topological phases also carries a nontrivial polarization which is quantized by the chiral symmetry. The polarization is given by,

$$P = \left[ \frac{1}{2\pi} \text{Im} \ln \det \mathcal{U} - \sum_{l,l',s,s'} \frac{X_{ls,l's'}}{2L} \right] \mod 1, \quad (5)$$

where the elements of  $\mathcal{U}$  read  $\mathcal{U}_{mn} \equiv \langle m|e^{i2\pi X/L}|n\rangle$ , and  $s, s' = A, B$  are the sublattice indices [62]. Due to its  $\mathbb{Z}_2$  nature, the polarization can only distinguishes between even or odd number of pairs of edge states.

We map out two typical phase diagrams in the  $R_x$ - $R_y$  plane according to the winding number and polarization, see Fig. 1(b) and 1(c). Numerical results clearly show the existence of the 0-type ( $\pi/T$ -type) amorphous SPT order with  $N_0 \approx 1$  ( $N_{\pi/T} \approx 1$ ) according to different driving conditions. Typically, we choose the periodic driving as  $\mathbf{f} = (0.9, 1, 1)$  to induce the 0-phase,

while  $\mathbf{f} = (1, 1, 0.55)$  to induce the  $\pi/T$ -phase, although in general the type of the Floquet SPT phase does not rely on the driving of certain components of  $\mathbf{R}$  (for more discussions, see Supplemental Material). Intuitively, as the driving period is increased such that the driving frequency is comparable to the band width, the  $\pi/T$ -gap would close and then reopen, which makes it possible to find the nontrivial  $\pi/T$  edge modes. In both nontrivial phase, the polarization is quantized to  $\approx 0.5$ , and showing the same phase boundaries with that predicted by the winding numbers. We note that the Floquet system can be topological even when both  $\hat{H}_1$  and  $\hat{H}_2$  are trivial. These results reveal the unique features of our model as a nonequilibrium system. Furthermore, We observe a clear deviation of the phase boundary compared to that in the regular limit. Part of the phase is trivial for regular system while becomes topological under structural disorder, which implies an amorphousness-driven phase transition in the Floquet system. We note that the conclusions are not limited for the stroboscopic driving. We also show that the SPT phase exists under hamornic driving in the Supplemental Material.

Figure 2 illustrates the typical 0-phase and  $\pi/T$ -phase transition event driven by the disorder. The phase transition is accompanied by gap closure. As shown in Fig. 2(b) and 2(e), the gap quickly drops as the disorder increases. We see that the energy gap decreases as the system size increases, indicating the gap closes in the thermodynamical limit and system enters a ungapped localization phase in the topological regime. The topology is protected by the mobility subgap rather than the spectral gap [63–66]. In such phase all states are localized. The localization properties are identified by both the level-spacing statistics and the mean inverse participation ratio (MIPR). For level statistics, we use the adjacent level-spacing ratio (LSR):  $r(\varepsilon) = [(1/(N_\varepsilon - 2)) \sum_i \min(\delta_i, \delta_{i+1}) / \max(\delta_i, \delta_{i+1})]$ , where  $\delta_i = \varepsilon_i - \varepsilon_{i-1}$  with eigen-quasienergies  $\varepsilon_i$ 's sorted in an ascending order, and  $N_\varepsilon$  is the number of the energy levels counted. As a general rule of thumb, for localized states,  $r \approx 0.386$ , fulfilling the Poisson statistics, whereas for extended states,  $r \approx 0.6$  associated with the Gaussian orthogonal ensemble. On another note, the MIPR is defined by  $I = \sum_{n,x} |\Psi_{n,x}|^4$  with  $|\Psi_{n,x}|^2$  being the local density of the  $n$ -th state on site  $x$ . A state is extended when  $I \sim 1/L$ . As comfired in Fig. 2(c) and 2(f), our model support robust ungapped 0-type and  $\pi$ -type localized SPT phase in a wide range of parameters, which is reminiscent of the Floquet Anderson insulator reported in Refs. [67, 68].

Next, we propose to detect the Floquet topological phases with microwave spectroscopy. To this end, a weak global microwave field with the Rabi frequency  $\Omega$  and detuning  $\Delta$  is shined on. Then the system is described by a Hamiltonian  $\hat{H}_\Omega = \hat{H} + \Omega/2 \sum_i (\hat{b}_i^\dagger + \hat{b}_i) - \Delta \sum_i \hat{b}_i^\dagger \hat{b}_i$ . The atoms are initially prepared in a vacuum state in

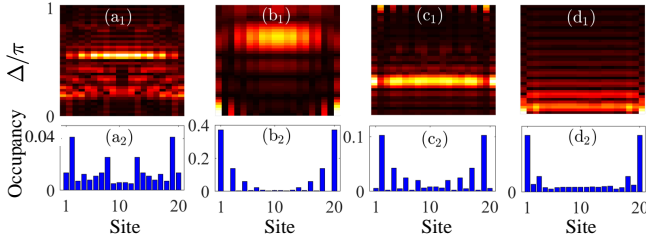


FIG. 3: Occupancy of each site excited by the microwave field with detuning  $\Delta$  for (a1)-(d1) and the corresponding selected Occupancy at  $\Delta = 0$  for (a2), (b2) and  $\Delta = \pi$  for (c2). We use  $\mathbf{R} = (-0.7, 0, 0.8)$ ,  $\mathbf{f} = (0.1, 1, 1)$ ,  $d = 0$ ,  $\Omega = 0.05$ ,  $t_m = 10T$  in (a);  $\mathbf{R} = (-0.5, 0, 0.8)$ ,  $\mathbf{f} = (0.7, 1, 1)$ ,  $d = 0$ ,  $\Omega = 0.05$ ,  $t_m = 30T$  in (b);  $\mathbf{R} = (-0.5, 0, 0.8)$ ,  $\mathbf{f} = (0.35, 1, 1)$ ,  $d = 0$ ,  $\Omega = 0.05$ ,  $t_m = 12T$  in (c);  $\mathbf{R} = (-0.9, 1.6, 0.8)$ ,  $\mathbf{f} = (0.5, 1, 1)$ ,  $d = 0.3$ ,  $\Omega = 0.05$ ,  $t_m = 60T$  in (d).

the s-level. After applying the microwave probe for some periods of time  $t_m$ , an excitation can be created only if an eigenstate energy matches the detuning  $\Delta$ . In Fig. 3, we display the site-resolved probability on the p-level at the final time for different configurations (trivial regular, topological 0-phase regular, topological  $\pi/T$ -phase regular, topological amorphous, respectively), which can be detected by the fluorescence imaging in the experiment. We can observe a clear signal of the edge mode at either zero or  $\pi$  detuning only in the topological phases, while a uniform distribution in the trivial cases.

*Many-body case.*—We now proceed to discuss the many-body case. The Hamiltonian (1) can be mapped to an XY spin model via Matsubara-Matsuda transformation,  $\hat{H}(t) = \sum_{i<j} V_{ij}(t)(\sigma_i^+ \sigma_j^- + \sigma_j^+ \sigma_i^-)$ , where  $\sigma_i^\pm = (\sigma_i^x \pm i\sigma_i^y)/2$  with  $\sigma_j^s$  ( $s = x, y, z$ ) being the Pauli matrices at site  $i$ . Correspondingly  $m_z = \sum_i \sigma_i^z/2$  is a conserved quantity. The subspace of the spin Hamiltonian with  $m_z = 0$  is equivalent to the hard-core bosonic Hamiltonian at half-filling. We note that the effective Hamiltonian containing longer-range hoppings, despite without an interaction term like  $\sigma_i^z \sigma_j^z$ , can not be cast to a free fermionic model by the inverse Jordan-Wigner transformation, showing the many-body aspect of our model.

We identify the topology of the many-body system by the topological entanglement entropy [69–71],

$$S_E = S_{L/2} + S_{\bar{L}/2} - S_{L/2 \cup \bar{L}/2} - S_{L/2 \cap \bar{L}/2}, \quad (6)$$

where  $S_{L/2}$  ( $S_{\bar{L}/2}$ ) is the half-chain entanglement entropy of the reduced density matrix for the left half (second quarter and fourth quarter) part of the chain. The phase diagram according to  $S_E$  is shown in Fig. 4(a). The TEE is calculated for a Floquet eigenstate (analogous to the ground state of a static system) of a second order effective Hamiltonian, which is not degenerate for system with a periodic boundary. For the many-body case, the quasi-energy will increase when more excitations are created,  $\varepsilon \sim \mathcal{O}(N)$ . Therefore, there exists larger parameter

regimes with  $\max(\varepsilon)T < 2\pi$  than the single particle case, where we could apply the Magnus expansion to simplify the numerical calculations. The TEE of a SPT states yields a quantized value  $2\ln 2$ , due to that the topology is essentially carried on the boundary. In contrast, TEE vanishes in the trivial phase. The numerical results show a robust region of the topological phase under structural disorder for the many body case. In addition, as an measurable signature of the Floquet SPT, we calculate the string order  $C_{\text{string}}^z = (-1)^{N-1} \langle \prod_{i=2}^{2L-1} \sigma_i^z \rangle$  [27, 72–74], in Fig. 4(b). The bulk of the topological states also acquire a finite long-range string order, and nearly vanishes in the trivial phase. We find that the TEE and the string order exhibit almost the same behaviors. In these calculations, We use ED for  $L < 10$  and DMRG for  $L > 10$ , and compare the results for different system sizes in Fig. 4(c).

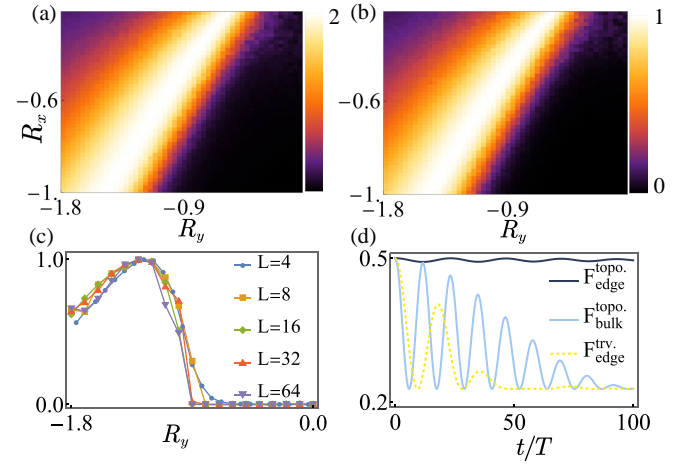


FIG. 4: (a) Phase diagram characterized by TEE  $S_E/\ln 2$  for a half-filled chain with  $2L = 8$  sites, and  $T_1 = T_2 = 0.4$ ,  $\mathbf{f} = (0.8, 1, 1)$ ,  $R_z = 0.55$ ,  $d = 0.8$ , and averaged over 100 random configurations. (b) Phase diagram characterized by string order, with same parameter setting. (c) String order for systems with different lattice size. We choose the section of  $R_x = -0.8$  here. (d) The trace fidelity for the topological case and trivial case for an amorphous lattice with  $2L = 12$  sites.

To further diagnose the boundary physics, we calculate the edge fidelity,  $F_z = \text{Tr}[\sigma_i^z(t)\sigma_i^z(0)]/N_{\text{dim}}$  with  $N_{\text{dim}}$  being the dimension of the Hilbert space, following the definition in Ref. [33]. The Floquet eigenstate is fourfold degenerate on open chains, as the edge modes for two sides can be either empty or occupied. As illustrated in Fig. 4(d), the edge sites exhibits much longer coherence time than the bulk sites only in the topological regime, but quickly damps in the trivial phase. The long edge coherence reveals the physical consequence of the SPT order in our model, and provides experimentally observable evidence.

*Discussions and conclusions.*—The topologically protected  $\pi/T$  quasienergy excitations in the Floquet sys-



tem always comes up in pairs, results in the subharmonic response at the edge [33, 75]. We show that our system exhibit time crystal behaviors at the edge sites, and such feature even exists under structural disorder. Although focused on the Rydberg atoms, our model may be generalized to other artificial quantum systems, such as trapped ion chain [76–79], and superconducting qubits [35, 36, 80]; and other symmetry class in higher dimensions.

In sumamry, we propose the Floquet SPT model in a 1D amorphous Rydberg tweezed array. We have study the topological properties in both single-particle and many-body levels. With various numerical calculations and careful comparision of different methods, the existence of rich Floquet SPT phases has been comfirmed. We have found that diverse exotic SPT phases can be induced from the trivial static system by the periodic driving, or from the regular system by the disorder, along with localization transition. We further addressed possible detection methods based on currently feasible technologies in the experimets of Rydberg atoms. Therefore, our work would provide a promising platform for exploring the exotic physics of noneuiblirium systemst hat are elusive in nature.

*Acknowledgments.*— This work was supported by the GRF (Grants No.17310622 and No.17303023) of Hong Kong.

---

\* Electronic address: [penghe@hku.hk](mailto:penghe@hku.hk)

† Electronic address: [wuh@cqupt.edu.cn](mailto:wuh@cqupt.edu.cn)

‡ Electronic address: [zwang@hku.hk](mailto:zwang@hku.hk)

- [1] M. Z. Hasan and C. L. Kane, Colloquium: topological insulators, *Rev. Mod. Phys.* **82**, 3045 (2010).
- [2] X.-L. Qi and S.-C. Zhang, Topological insulators and superconductors, *Rev. Mod. Phys.* **83**, 1057 (2011).
- [3] C. K. Chiu, J. C. Teo, A. P. Schnyder, and S. Ryu, Classification of topological quantum matter with symmetries, *Rev. Mod. Phys.* **88**, 035005 (2016).
- [4] D.-W. Zhang, Y.-Q. Zhu, Y.-X. Zhao, H. Yan, and S.-L. Zhu, Topological quantum matter with cold atoms, *Adv. Phys.* **67**, 253 (2018).
- [5] N. P. Armitage, E. J. Mele, and A. Vishwanath, Weyl and Dirac semimetals in three-dimensional solids, *Rev. Mod. Phys.* **90**, 015001 (2018).
- [6] Y. Xu, Topological gapless matters in three-dimensional ultracold atomic gases, *Front. Phys.* **14**, 43402 (2019).
- [7] S. Aubry and G. André, Analyticity breaking and Anderson localization in incommensurate lattices, *Ann. Isr. Phys. Soc.* **3**, 133 (1980).
- [8] P. G. Harper, Single band motion of conduction electrons in a uniform magnetic field, *Proc. Phys. Soc. London Sect. A* **68**, 874 (1955).
- [9] S. Das Sarma, S. He, and X. C. Xie, Localization, mobility edges, and metal-insulator transition in a class of one-dimensional slowly varying deterministic potentials, *Phys. Rev. B* **41**, 5544 (1990).
- [10] J. Biddle and S. Das Sarma, Predicted mobility edges in one-dimensional incommensurate optical lattices: An exactly solvable model of Anderson localization, *Phys. Rev. Lett.* **104**, 070601 (2010).
- [11] P. Corbae, J. D. Hannukainen, Q. Marsal, D. Muñoz-Segovia, and A. G. Grushin, Amorphous topological matter: Theory and experiment, *Europhys. Lett.* **142**(1), 16001 (2023).
- [12] A. Agarwala and V. B. Shenoy, Topological insulators in amorphous systems, *Phys. Rev. Lett.* **118**, 236402 (2017).
- [13] Y. B. Yang, T. Qin, D. L. Deng, L.-M. Duan, and Y. Xu, Topological amorphous metals, *Phys. Rev. Lett.* **123**, 076401 (2019).
- [14] J. H. Wang, Y. B. Yang, N. Dai, and Y. Xu, Structural-disorder-induced second-order topological insulators in three dimensions, *Phys. Rev. Lett.* **126**, 206404 (2021).
- [15] M. N. Ivaki, I. Sahlberg, and T. Ojanen, Criticality in amorphous topological matter: Beyond the universal scaling paradigm, *Phys. Rev. Res.* **2**, 043301 (2020).
- [16] I. Sahlberg, A. Westström, K. Pöyhönen, and T. Ojanen, Topological phase transitions in glassy quantum matter, *Phys. Rev. Res.* **2**, 013053 (2020).
- [17] J. D. Hannukainen, M. F. Martínez, J. H. Bardarson, and T. K. Kivring, Local topological markers in odd spatial dimensions and their application to amorphous topological matter, *Phys. Rev. Lett.* **129**, 277601 (2022).
- [18] C. Wang, T. Cheng, Z. Liu, F. Liu, and H. Huang, Structural amorphization-induced topological order, *Phys. Rev. Lett.* **128**, 056401 (2022).
- [19] X. Cheng, T. Qu, L. Xiao, S. Jia, J. Chen, and L. Zhang, Topological Anderson amorphous insulator, *Phys. Rev. B*, **108**, L081110 (2023).
- [20] T. Kitagawa, E. Berg, M. Rudner, and E. Demler, Topological characterization of periodically driven quantum systems, *Phys. Rev. B* **82**, 235114 (2010).
- [21] M. S. Rudner, N. H. Lindner, E. Berg, and M. Levin, Anomalous edge states and the bulk-edge correspondence for periodically driven two dimensional systems, *Phys. Rev. X* **3**, 031005 (2013).
- [22] N. Goldman and J. Dalibard, Periodically Driven quantum systems: effective Hamiltonians and engineered gauge fields, *Phys. Rev. X* **4**, 031027 (2014).
- [23] A. Eckardt, Colloquium: Atomic quantum gases in periodically driven optical lattices, *Rev. Mod. Phys.* **89**, 011004 (2017).
- [24] R. Roy and F. Harper, Periodic table for Floquet topological insulators, *Phys. Rev. B* **96**, 155118 (2017).
- [25] S. Yao, Z. Yan, Z. Wang, Topological invariants of Floquet systems: General formulation, special properties, and Floquet topological defects, *Phys. Rev. B* **96**, 195303 (2017).
- [26] F. D. M. Haldane, Nonlinear field theory of large-spin Heisenberg antiferromagnets: semiclassically quantized solitons of the one-dimensional easy-axis Néel state, *Phys. Rev. Lett.* **50**, 1153 (1983).
- [27] F. Pollmann, A. M. Turner, E. Berg, M. Oshikawa, Entanglement spectrum of a topological phase in one dimension, *Phys. Rev. B* **81**, 064439 (2010).
- [28] X. Chen, Z.-C. Gu, and X.-G. Wen, Classification of gapped symmetric phases in one-dimensional spin systems, *Phys. Rev. B* **83**, 035107 (2011).
- [29] X. Chen, Z.-C. Gu, Z.-X. Liu, and X.-G. Wen, Symmetry-

- protected topological orders in interacting bosonic systems, *Science* **338**, 1604–1606 (2012).
- [30] V. Khemani, A. Lazarides, R. Moessner, and S. L. Sondhi, Phase structure of driven quantum systems, *Phys. Rev. Lett.* **116**, 250401 (2016).
- [31] A. C. Potter, T. Morimoto, and A. Vishwanath, Classification of interacting topological Floquet phases in one dimension, *Phys. Rev. X* **6**, 041001 (2016).
- [32] H. C. Po, L. Fidkowski, T. Morimoto, A. C. Potter, and A. Vishwanath, Chiral Floquet phases of many-body localized bosons, *Phys. Rev. X* **6**, 041070 (2016).
- [33] I. D. Potirniche, A. C. Potter, M. Schleier-Smith, A. Vishwanath, and N. Y. Yao, Floquet symmetry-protected topological phases in cold-atom systems, *Phys. Rev. Lett.* **119**, 123601 (2017).
- [34] F. Harper, R. Roy, Floquet topological order in interacting systems of bosons and fermions, *Phys. Rev. Lett.* **118**, 115301 (2017).
- [35] F. Mei, Q. Guo, Y.-F. Yu, L. Xiao, S.-L. Zhu, and S. Jia, Digital simulation of topological matter on programmable quantum processors, *Phys. Rev. Lett.* **125**, 160503 (2020).
- [36] X. Zhang, W. Jiang, J. Deng, et al., Digital quantum simulation of Floquet symmetry-protected topological phases, *Nature* **607**, 468–473 (2022).
- [37] M. Saffman, T. G. Walker, and K. Mølmer, Quantum information with Rydberg atoms, *Rev. Mod. Phys.* **82**, 2313 (2010).
- [38] A. Browaeys and T. Lahaye, Many-body physics with individually controlled Rydberg atoms, *Nat. Phys.* **16**, 132 (2020).
- [39] S. Geier, N. Thaicharoen, C. Hainaut, et al., Floquet Hamiltonian engineering of an isolated many-body spin system, *Science* **374**, 1149 (2021).
- [40] P. Scholl, H. J. Williams, G. Bornet, et al., Microwave Engineering of Programmable XXZ Hamiltonians in Arrays of Rydberg Atoms, *PRX Quantum* **3**(2): 020303 (2022).
- [41] T.-F. J. Poon, X.-C. Zhou, B.-Z. Wang, T.-H. Yang, and X.-J. Liu, Fractional quantum anomalous Hall phase for Raman superarray of Rydberg atoms, *Adv Quantum Technol.*, 2300356 (2024).
- [42] Y. Cheng and H. Zhai, Emergent gauge theory in Rydberg atom arrays, *arXiv:2401.07708* (2024).
- [43] M. Endres, H. Bernien, A. Keesling, H. Levine, E. R. Anschuetz, A. Krajenbrink, C. Senko, V. Vuletic, M. Greiner, and M. D. Lukin, Atom-by-atom assembly of defect-free one-dimensional cold atom arrays, *Science* **354**, 1024 (2016).
- [44] H. Kim, W. Lee, H.-g. Lee, H. Jo, Y. Song, and J. Ahn, In situ single-atom array synthesis using dynamic holographic optical tweezers, *Nat. Commun.* **7**, 13317 (2016).
- [45] D. Barredo, S. De Léséleuc, V. Lienhard, T. Lahaye, and A. Browaeys, An atom-by-atom assembler of defect-free arbitrary two-dimensional atomic arrays, *Science* **354**, 1021 (2016).
- [46] D. Barredo, V. Lienhard, S. De Léséleuc, T. Lahaye, and A. Browaeys, Synthetic three-dimensional atomic structures assembled atom by atom, *Nature* **561**, 79 (2018).
- [47] A. Browaeys, D. Barredo, T. Lahaye, Experimental investigations of dipole–dipole interactions between a few Rydberg atoms, *J. Phys. B* **49**, 152001 (2016).
- [48] A. P. Orioli, A. Signoles, H. Wildhagen, G. Günter, J. Berges, S. Whitlock, and M. Weidemüller, Relaxation of an isolated dipolar-interacting Rydberg quantum spin system, *Phys. Rev. Lett.* **120**, 063601 (2018).
- [49] A. Signoles, T. Franz, R. Ferracini Alves, M. Gärttner, S. Whitlock, G. Zürn, and M. Weidemüller, Glassy Dynamics in a disordered Heisenberg quantum spin system, *Phys. Rev. X* **11**, 011011 (2021).
- [50] S. de Léséleuc, V. Lienhard, P. Scholl, D. Barredo, S. Weber, N. Lang, H. P. Büchler, T. Lahaye, and A. Browaeys, Observation of a symmetry-protected topological phase of interacting bosons with rydberg atoms, *Science* **365**, 775 (2019).
- [51] V. Lienhard, P. Scholl, S. Weber, et al., Realization of a density-dependent Peierls phase in a synthetic, spin-orbit coupled Rydberg system, *Phys. Rev. X* **10**, 021031 (2020).
- [52] D. Bluvstein, A. Omran, H. Levine, et al., Controlling quantum many-body dynamics in driven Rydberg atom arrays, *Science* **371**, 1355–1359 (2021).
- [53] G. Semeghini, H. Levine, A. Keesling, S. Ebadi, T. T. Wang, D. Bluvstein, R. Verresen, H. Pichler, M. Kalinowski, R. Samajdar, et al., Probing topological spin liquids on a programmable quantum simulator, *Science* **374**, 1242 (2021).
- [54] C. Chen, G. Bornet, M. Bintz, G. Emperauger, L. Leclerc, V. S. Liu, P. Scholl, D. Barredo, J. Hauschild, S. Chatterjee, et al., Continuous symmetry breaking in a two-dimensional rydberg array, *Nature* **616**, 691 (2023).
- [55] S. Julià-Farré, J. Vovrosh, A. Dauphin, Amorphous quantum magnets in a two-dimensional Rydberg atom array, *arXiv:2402.02852* (2024).
- [56] K. Li, J. H. Wang, Y. B. Yang, and Y. Xu, Symmetry-protected topological phases in a Rydberg glass, *Phys. Rev. Lett.* **127**, 263004 (2021).
- [57] H. Wu and J. H. An, Floquet topological phases of non-Hermitian systems, *Phys. Rev. B* **102**, 041119 (2020).
- [58] A. Kitaev, Anyons in an exactly solved model and beyond, *Ann. Phys. (Amsterdam)* **321**, 2 (2006).
- [59] R. Bianco and R. Resta, Mapping topological order in coordinate space, *Phys. Rev. B* **84**, 241106(R) (2011).
- [60] L. Lin, Y. Ke, and C. Lee, Real-space representation of the winding number for a one-dimensional chiral-symmetric topological insulator, *Phys. Rev. B* **103**, 224208 (2021).
- [61] L. Zhou and J. Gong, Non-Hermitian Floquet topological phases with arbitrarily many real-quasienergy edge states, *Phys. Rev. B* **98**, 205417 (2018).
- [62] R. Resta, Quantum-mechanical position operator in extended systems, *Phys. Rev. Lett.* **80**, 1800 (1998).
- [63] Y. Y. Zhang, R. L. Chu, F. C. Zhang, and S. Q. Shen, Localization and mobility gap in topological Anderson insulator, *Phys. Rev. B* **85**, 035107 (2012).
- [64] T. A. Loring, K-theory and pseudospectra for topological insulators, *Annals of Physics* **356**, 383–416 (2015).
- [65] A. Cerjan and T. A. Loring, Local invariants identify topology in metals and gapless systems, *Phys. Rev. B* **106**, 064109 (2022).
- [66] M. Ren, Y. Yu, B. Wu, et al., Realization of gapped and ungapped photonic topological Anderson insulators, *Phys. Rev. Lett.* **132**, 066602 (2024).
- [67] P. Titum, N. H. Lindner, M. C. Rechtsman, and G. Refael, Disorder-induced Floquet topological insulators, *Phys. Rev. Lett.* **114**, 056801 (2015).
- [68] P. Titum, E. Berg, M. S. Rudner, G. Refael, and N. H. Lindner, Anomalous Floquet-Anderson insulator as a

- nonadiabatic quantized charge pump, *Phys. Rev. X* **6**, 021013 (2016).
- [69] B. Zeng and X.-G. Wen, Gapped quantum liquids and topological order, stochastic local transformations and emergence of unitarity, *Phys. Rev. B* **91**, 125121 (2015).
- [70] B. Zeng and D. L. Zhou, Topological and error-correcting properties for symmetry-protected topological order, *Europhysics Letters* **113**, 56001 (2016).
- [71] H. Ling, P. Richard, S. R. Koshkaki, M. Kolodrubetz, D. Meidan, A. Mitra, T. Pereg-Barnea, Disorder induced topological phase transition in a driven Majorana chain, *arXiv:2310.17088* (2023).
- [72] M. den Nijs and K. Rommelse, Preroughening transitions in crystal surfaces and valence-bond phases in quantum spin chains, *Phys. Rev. B* **40**, 4709 (1989).
- [73] T. Kennedy and H. Tasaki, Hidden  $Z_2$  symmetry breaking in Haldane-gap antiferromagnets, *Phys. Rev. B* **45**, 304 (1992).
- [74] K. Hida, Ground-state phase diagram of the spin-1/2 ferromagnetic antiferromagnetic alternating Heisenberg chain with anisotropy. *Phys. Rev. B* **46**, 8268 (1992).
- [75] R. W. Bomantara, S. Mu, and J. Gong, Topological and dynamical features of periodically driven spin ladders, *Phys. Rev. B* **103**, 235404 (2021).
- [76] S. L. Zhu, C. Monroe, and L.M. Duan, Trapped ion quantum computation with transverse phonon modes, *Phys. Rev. Lett.* **97**, 050505 (2006).
- [77] R. Blatt and C. F. Roos, Quantum simulations with trapped ions, *Nat. Phys.* **8**, 277 (2012).
- [78] J. Zhang, et al. Observation of a discrete time crystal. *Nature* **543**, 217 (2017).
- [79] A. Kyprianidis, et al., Observation of a prethermal discrete time crystal. *Science* **372**, 1192 (2021).
- [80] C. Ying, et al., Floquet prethermal phase protected by  $u(1)$  symmetry on a superconducting quantum processor, *Phys. Rev. A* **105**, 012418 (2022).